Available online at www.dergipark.org.tr/en

INTERNATIONAL ADVANCED RESEARCHES and ENGINEERING JOURNAL

Journal homepage: www.dergipark.org.tr/en/pub/iarej

e-ISSN: 2618-575X

International Open Access

Volume 08
Issue 03

December, 2024

Research Article

Investigation of microstructure and microhardness properties of Nd: YAG laser welded galvanized steel plates

Arife Kübra Yontar [a,*] ***and Sinem Çevik*** [b]

[a]*Department Mechanical and Metal Technologies, Ondokuz Mayis University, 55300, Samsun, Turkey*
[b]*Department of Metallurgical and Materials Engineering, Ondokuz Mayis University, 55270, Samsun, Turkey*

ARTICLE INFO

Article history:
Received 02 September 2024
Accepted 02 December 2024
Published 20 December 2024

Keywords:
Galvanized Steel
Laser Welding
Microhardness
Microstructure

ABSTRACT

Modern industry has discovered many uses for stainless steel because of its excellent mechanical and physical qualities, outstanding resistance to oxidation and corrosion, hot and cold workability, and superior weldability. The development of lightweight, cost-effective materials is being driven by technological advances. Thus, in order to satisfy Industry 4.0 criteria, additional materials that are resistant to corrosion and oxidation are required. Utilizing galvanization has extended the lifespan of materials used in the chemical, automotive, and white goods sectors, among other industries. Zinc coating, often known as galvanizing, is one technique for surface protection. It is inevitable that welding techniques will become widely used in component manufacturing. Several welding techniques may be used on galvanized materials, but they also come with several drawbacks for the joined samples, including flaws, porosities, and solidification fissures. As a result, the popularity of laser welding (LW) has steadily risen. In the current research, Nd-YAG laser welding was used to combine 2mm thick sheet-galvanized steel sheets. Microhardness tests were used to assess welded samples to determine their mechanical characteristics. Experimental results showed that the microhardness of the welded area was higher than that of the base metal. The microstructure of the welded samples was also examined using SEM and EDS mapping to look for flaws in the base metal, coating, welded area, and HAZ. SEM images revealed that a martensite structure was formed in the weld area, and a smooth joining process was achieved.

1. Introduction

New and innovative welding methods are becoming more and more necessary as technology advances rapidly. When deciding on a welding joint method to utilize, consideration is given to factors such as cost, quality, automation, and time efficiency. The ability of welded joints to meet requirements including self-attraction, impact resistance, corrosion resistance, and strength properties-as well as pre-, intermediate, and final annealing-is crucial. Aside from these, factors including investment costs, operational and consumable expenses, and the choice and application of filler metal are considered when determining the best technique to utilize [1, 2].

Gas tungsten arc welding (GTAW) is a common industrial technique for joining nearly any metallic material, including stainless steel, aluminum, nickel, and nickel alloys. Between the tungsten electrode and the sample in GTAW, an arc is created by a combination of argon, helium, or all shielding gas burning freely [3, 4]. GTAW welding has some disadvantages, such as the mixing of the tungsten electrode with the weld bead, oxide residues, pore formation, insufficient melting, and the formation of end crater cracks [5–7].

The joining procedures must be extended to lower dimensions due to the constant condition of the gadget parts. Conventional welding techniques are not applicable when small-sized items are employed in production settings. The most effective joining technique available today is laser beam welding, an advanced method whose benefits include deep penetration, low heat input, fast welding speed, negligible distortion, and use in an aqueous environment [8, 9]. The low energy input and high joint strength of the material to be welded makes it attractive since the heat in the weld zone has less of an effect on it. The base material's microstructure changes minimally due to the low linear energy input, which produces a smaller weld zone and heat-affected zone (HAZ).

* Corresponding author. Tel.: +*903623121919*
E-mail addresses: kubra.demirbas@omu.edu.tr *(A.K. Yontar)*, sinemu@omu.edu.tr *(S. Çevik)*
ORCID: 0000-0003-1486-9332 *(A.K. Yontar)*, 0000-0002-3506-7892 *(S. Çevik)*
DOI: 10.35860/iarej.1541710

Its additional features are its excellent power density and outstanding focusability in the few nanometer regions. The ability of the lens to focus light on focal points smaller than 0.005 inches makes the lens's participation in this process crucial [10–12]. The advantages of laser welding are its fast speed, limited heat-affected zone, deep penetration, high-quality welding joints, low heat input per unit volume, dispersion of fiber optic beams, and ease of robot operation [13]. A few milliseconds is all that is needed as a welding time to achieve high production rates and avoid metallurgical internal structural changes. Since shielding gas and a vacuum environment are not needed for the generation of laser beams, they provide substantial cost and speed benefits, particularly in mass production. As a result, laser welding makes combining tiny, thin parts feasible to create a narrow, smooth weld seam [14–16]. The laser source works on the concept that light energy is transformed into heat energy on the component's surface to be welded when the focal point is aimed. Before the heat-affected zone (HAZ) forms, the piece's outer layer starts to melt, and condensed energy facilitates melting and bonding [17].

1.06 micron light is produced using a neodymium-YAG solid-state laser, which employs an industrial crystal as its active substrate. It can run on beam powers ranging from around 100W to 3kW. Nd: YAG solid-state lasers can produce 10-kW brief pulses despite having lower average powers than CO_2 gas lasers. The 1kW Nd: YAG laser equipment can weld 4mm thick steel forehead at a pace of 0.3 meters per minute with great speed. The most significant benefit is that, because of the wavelength of the laser beam it generates, it makes control easier by allowing energy to be sent across fiber optic cables [18, 19].

Due to their excellent corrosion resistance, galvanized steels have seen significant growth in application in the automobile sector in the last decade. Galvanized steels exhibit high performance in both low and high-temperature service situations. As per the findings of other steels, vehicles with galvanized steels have lower weights and, thus, use less gasoline. Thus, cost-effective manufacture and increased vehicle safety may be guaranteed [20–22]. Galvanization is a commonly employed technique that involves applying a zinc coating to the surface of steel in order to prevent the effects of corrosion. By submerging the iron and steel in the molten zinc bath, zinc, and zinc compounds are often present in many layers of this protective coating. Galvanizing modifies the intricate structure of the layers, which has an impact on characteristics like chemical activity, diffusion, and subsequent cooling [23–25]. It is common practice to join galvanized steel using conventional welding techniques, which are identical to those employed for joining noncoated steel. Zinc is not as soluble as steel, though, and it has a lower melting point. Steel begins to melt around 1809 K, whereas zinc vaporizes at 1180 K thermal temperature [26]. Because of this, zinc burns during the welding process, resulting in porosity, various flaws, fractures, HAZ softening, and zinc depletion in the weld zone. Laser welding is an excellent approach to combining galvanized steel to prevent these unwanted issues. Because flaws, fractures, and porosities reduce the weld seam's mechanical strength, which is unacceptable in many applications. Therefore, in order to generate high-quality weldments, further study and developments for the joining of galvanized steels by laser welding are required [27–30].

The present study investigated the weldability of galvanized steel, which was joined by the Nd- YAG laser welding method. The microstructural examination of the welded specimens is carried out with the optical microscope and SEM/ EDS analyses. The hardness of the laser welded specimens is measured with the Vickers hardness tester.

2. Materials And Methods

2.1 Preparation of galvanized steel plates

The galvanized steel sheet with a length of 10 cm and a thickness of 2 mm was cut into ten equal pieces with the SRGM 1360-SAYMAK cutting device shown in Figure 1(a). The simulated and authentic appearance of the samples prepared before welding are shown in Figures 2(b) and (c).

2.2 Nd: YAG laser welding of galvanized steels

The experiments focused on laser welding with a solid-state Nd: YAG-laser. 1470 watts of power were used, and the focal length was over 0 to 15 and 20 mm in travel speeds. As maximum output power, 4 kW is used. All parameters used in the welding application are given in Table 1. When butt welding, especially in butt welding of galvanized steels, the gap between the samples must be adjusted precisely one hand, issues such as porosity and discontinuity in welding joints can be readily generated if the sheets are firmly secured together due to the notable difference between the melting temperature of steel (1583° C) and the zinc's evaporation temperature (906° C). However, excessive gaps result in poor weld appearance and, in certain situations, even impair the ability of the workpieces to be effectively integrated into one another. According to Mei et.al.(2009) [13], the gap should be controlled within 10% of the thickness of the workpiece in deep-penetration laser welding. Considering all of those affecting factors, while the workpieces are fixed, the gap between workpieces should be controlled within 0.15–0.2 mm. The appearance of samples after welding is shown in Figure 2 (a).

Four total samples were prepared by cutting the laser-welded specimens into tiny pieces with a 0.5–1 cm diameter to confine the weld zone for the optical microscope and hardness tests. After sanding and etching, the mounted

samples were evaluated under an optical microscope. The etching solution consisted of 20 mL of ethanol, 20 mL of hydrochloric acid, and one gram of cuprous chloride dihydrate solution. Images of metallographically prepared samples are shown in Figure 2 (b).

Table 1. Welding parameters.

Flow Rate	6-7 L/dk
Current Setting	60-70 A
Gas Type	Argon
Gas Setting	1.2 L
Angle Between Metal-Piece	20°

2.3 Characterizations

The stereo microscope (Leica DM2500 P) was used to evaluate the microstructure and the defect distribution of the polished surface of the welded specimen. The hardness values of the samples were measured at 3 mm intervals by applying a force of 0.98 kg for 15 seconds using the TMTECK HV-1000B Micro hardness device. The effect of the welding process on the hardness of the alloy was examined by comparing the hardness values of the welding zone, the heat-affected zone, and the base metal zone. A JEOL 7001F field emission (FE) scanning electron microscope with an EDS attachment and an 80mm^2 X-MAX detector was used to investigate the substances' microstructural characterization and EDS chemical mapping. A Scanning Electron Microscope (SEM) examination was conducted for every Nd: YAG laser-welded specimen. Energy-dispersive spectroscopy (EDS) was used to analyze materials semiquantitatively chemically. The compositions of the welded samples were determined through map analysis and EDS spectra. Thus, research is done on how many elements, including zinc vaporization, shielding gas, welding speed, laser power, and focal location, affect the quality of the welded joints. The behavior of the weld pool during zero-gap and butt laser welding was thoroughly investigated.

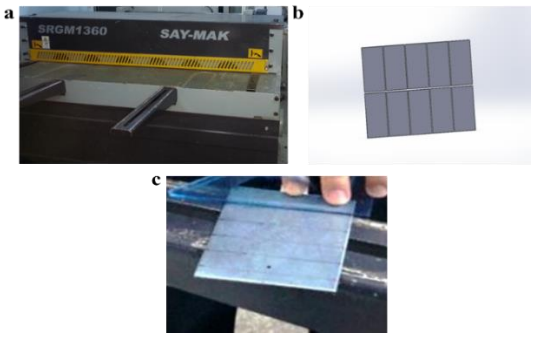

Figure 1. (a) Cutting Device, (b) simulation of samples prepared before cutting, and (c) galvanized steel plate prepared for cutting.

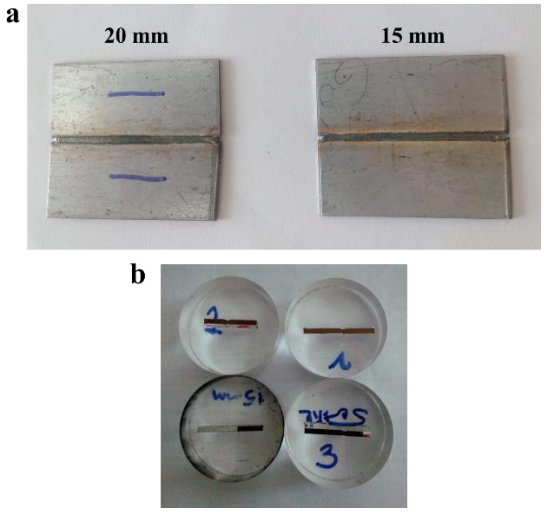

Figure 2. (a) Nd: YAG laser welded samples and (b) metallographically prepared samples.

3. Results And Discussion

3.1 Optical Microscope Analysis

The optical microscope images in Figure 3 clearly show that the laser-welded steel has a smooth and homogeneous structure. It is also seen that the plates of the same thickness, which are joined together with the laser welding, are uniform and smooth. The galvanized steel joined by the laser welding method has a crack-free, fault-free welding appearance in HAZ. It is obvious that the welded area of the sample joined with a 15 mm focal length, shown in Figure 3 (a), is broader and more uniform. However, the sample with a 20 mm focal length does not have pores, indicating that the joint is of higher quality and more integrated. As shown in Figures 3 (a) and (b), excessive grain growth is not a concern in the HAZ of laser-welded specimens. This shows us that both welded joints have no negative effect on toughness and deformability.

It is crucial to consider how the laser's power affects the weld's width and depth. As laser power increases, the weld's depth and breadth also rise [13]. This is due to the fact that when laser power grows, so does the quantity of heat input. The laser may achieve complete penetration when its power exceeds 1300W. The aspect ratio of the weld joint falls, and the increasing rate for the depth and width of the weld seam is less than that for the width of the weld seam when the laser power exceeds 1300W. As a result, in the current investigation, an adequate laser power of around 1470 W is used. As well known, the keyhole effect is the essential characteristic of deep-penetration laser welding, which plays a vital role in the energy coupling during the welding process [31, 32]. Therefore, this effect can be clearly seen in Figure 3.

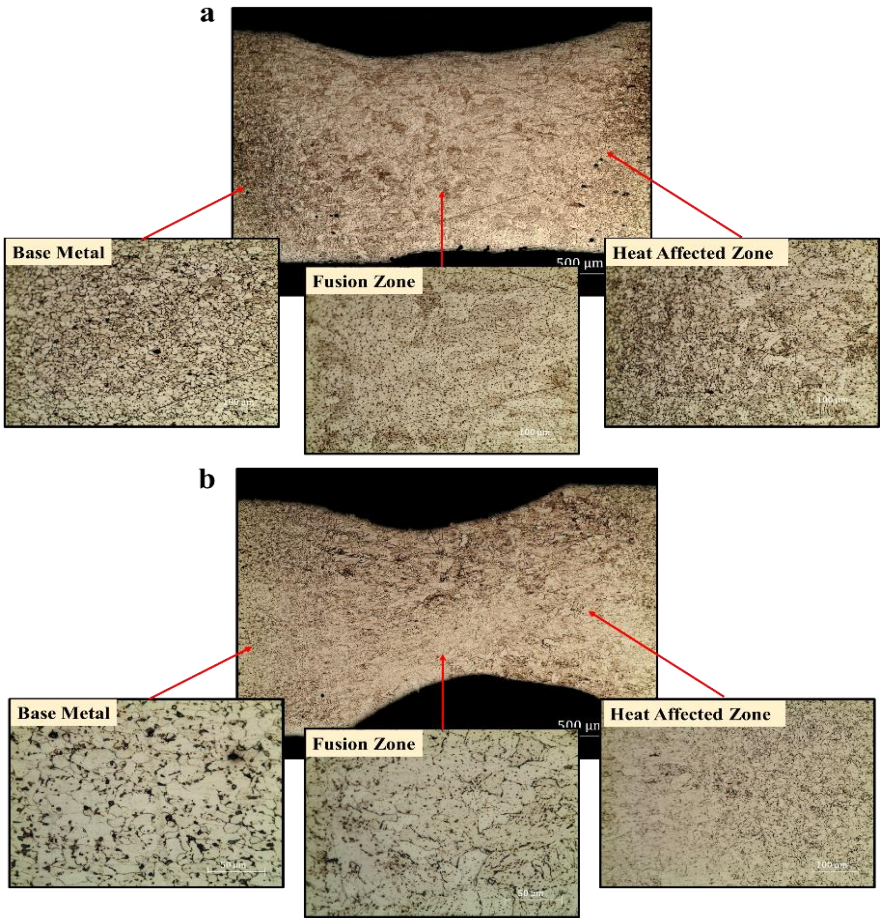

Figure 3. Optical microscope images of (a) steel sample welded with laser at 15 mm focal length and (b) steel sample welded with 20 mm focal length.

3.2 SEM and EDS analyses

When the laser power is greater than 1200W, some very small pores are observed in HAZ, as shown in Figure 4(a) HAZ image. As laser power drops, the number of pores falls as well. Low laser power is claimed to be able to prevent pore development by lowering the generation of metal vapor. Zinc vaporization is one of the main factors boosting splashing electric spark and porosity during laser welding of galvanized steel sheets. On the other hand, rapid zinc evaporation lowers the amount of zinc in the welding joint, and HAZ expands the hazardous area, weakens welding stability, and ruins the galvanized layer, all of which will eliminate the galvanized steel's protective layer. Furthermore, quick zinc vaporization lowers the quality of welding connections, creates internal tension, pores, and cracks in the joints, and makes safeguarding focusing mirrors more challenging. Shielding gas serves several crucial purposes in high-power deep-penetration laser welding, including preventing oxidation of the workpiece surface, ensuring that zinc vapor has no effect, suppressing the creation of pores, and clearing the plasma cloud that absorbs and disperses laser energy. Plasma can be restrained to reduce the strength of the plasma density by choosing the suitable shielding gas. Appropriate plasma in the keyhole is beneficial to improve the workpiece's absorption of laser energy and, therefore, boost weld penetration. The side-blow shielding gas used in this investigation to protect the welding joints is argon (Ar). In a high-temperature melt pool, nitrogen (N_2) causes a metallurgical reaction with a base metal substance [33–35]. Nitrogen, a comparatively reactive gas, can react with the weld metal when utilized as a shielding gas because it dissolves in the pool at high temperatures. Instead of reacting with the base metal, argon is an inert gas. Consequently, nitrogen has a far deeper penetration depth than argon does. Porosity and nitride, however, appear in the welds because nitrogen molecules can split into nitrogen atoms (N_2- 2[N]). Since the weld metal has porosity, the nitrogen can achieve the ideal penetration criterion but not the formability criteria [36]. Ar is selected as shielding gas during the welding process to obtain better manufacturing performance for tailor-welded sheets. So, no deformation, distortion, porosities, or failures are observed in the fusion zone and base metal of samples seen in Figure 4. Heat-induced decomposition of moisture that is either adhered to the workpiece surface or present in the ambient into hydrogen can result in the creation of pores in welding joints. It can be seen that after taking these measures, the welding joints are of high quality and practically free of pores, as shown in Figure 4.

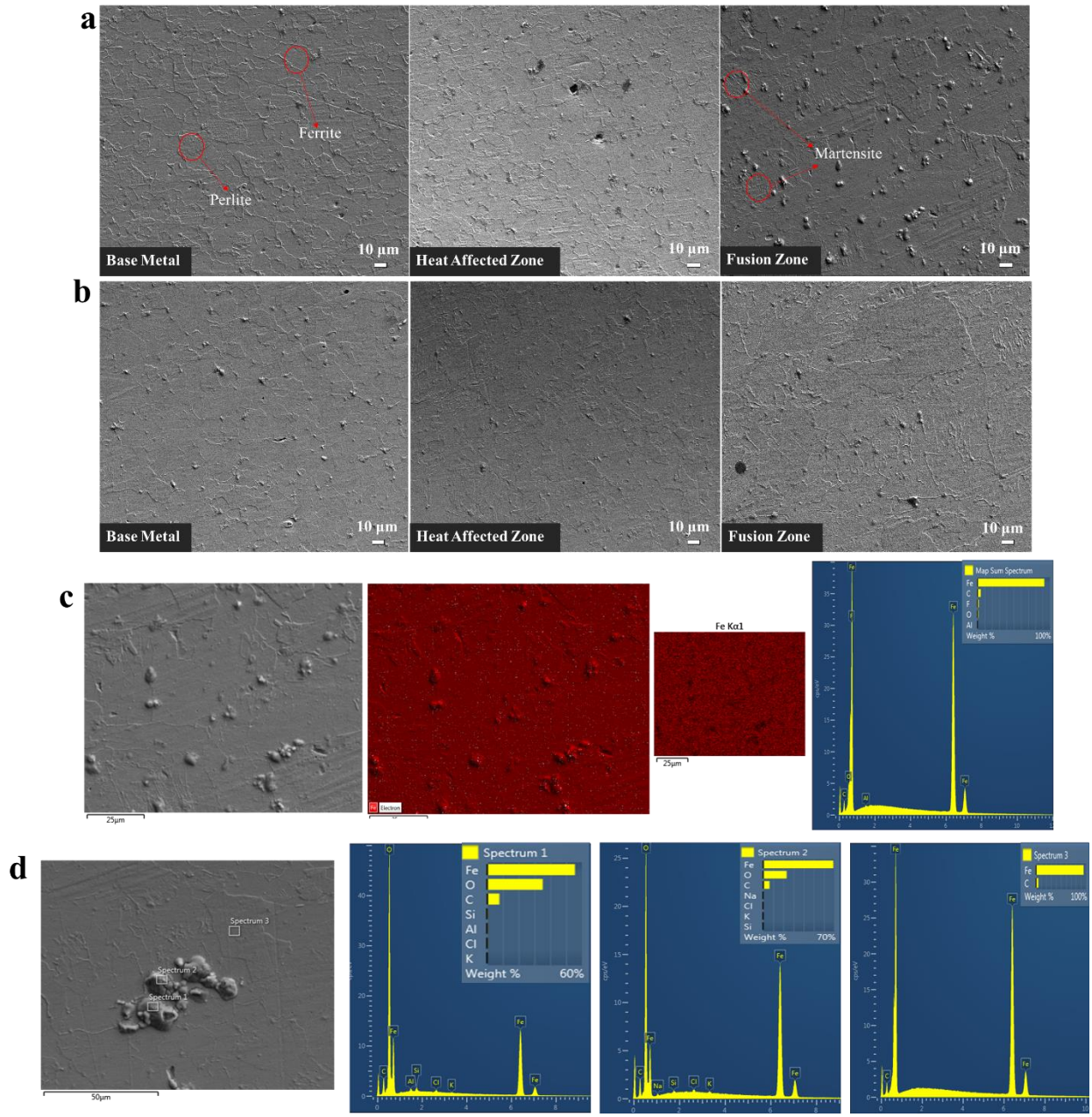

Figure 4. SEM images of (a) 15 mm focal length welded sample, (b) 20 mm focal length welded sample, EDS results of (c) 15 mm focal length welded sample, (d) 20 mm focal length welded sample.

As seen in Figure 4 (a) and (b), the base metal consists of ferrite and pearlite, which is a typical steel microstructure [37]. It is understood that the grains grow as we move from the base metal to the heat-affected zone (HAZ) and the weld zone. As is known, when metals are heated to a temperature above the recrystallization temperature, a phenomenon called grain growth occurs. The grain growth rate increases as the temperature increases, and the growth accelerates as the solidus of the metal approaches. Coarse-grained structures are more brittle and fragile than fine-grained structures [38–40]. Figure 4 shows an island of martensite in the weld regions, typically expected due to the rapid cooling rates inherent in the laser welding process. A coarser martensite structure formed after cooling as a result of the austenite's more immense grain development produced by the higher peak temperature [40, 41].

Energy-dispersive X-ray Spectroscopy (EDS) was used to detect the atomic percent of the zinc and the iron distribution in the preheated zone and the welds. Also, in order to determine the changes in the chemical composition of the material caused by the influence of the laser beam, the distribution of elements in different zones in deep-penetration laser welds is tested by EDS/SEM. It can be seen in Figures 4 (c) and (d) because, compared to base metal, the elements and their atomic fraction in welding joints have changed accordingly. Factors such as Si, C, O, and Fe exhibit

varying degrees of fluctuation in distribution from the welding joint to the base metal. This helps to explain why the elements in welding joints differ from those in the base metal. The equilibrium in the fusion zone's crystallization mechanism is the cause, and the fast cooling rate of welding joints results in insufficient phase transition and diffusion of alloy components. Thus the solute element deviates from its average density due to the unequal chemical composition distributions. If the welding speed is too fast, the time for the melt pool to resolidify is short, making it easy to produce pores in welding joints due to the zinc vaporization during welding [42–44]. Since the amount of zinc was very low and evaporation occurred during the welding process, Zn element was not detected in the EDS results.

3.3 Micro Vickers Hardness

The butt welding Nd: YAG-laser welding of Vicker's micro-hardness measurement was carried out in order to determine the hardness distribution profiles along the weld zone, heat-affected zone (HAZ), and base metal. As can be seen from Figure 5 (b) and (c), the Vickers hardness values were measured by applying a force at a total of 15 points at intervals of 0.5 mm from the two sides of the welding region of the samples. The martensitic transformation in the weld zone and in the heat-affected zone increases the hardness in the zones compared to the hardness of the base metal. The increased hardness in the welding zone can be attributed to re-austenitization and the formation of a martensitic structure upon cooling [41]. The hardness results graph given in Figure 5 (a) shows that the hardness value of the weld zone is harder than the base metal and HAZ for the three samples due to the martensitic transformation of the grains. Samples G 15.1 and G 15.2 are laser-welded samples with a focal length of 15 mm. Samples G 20.1 and G 20.2 are laser-welded samples with a focal length of 20 mm. According to the study, the galvanized steel joined by laser welding has a smoother weld zone, and microstructural examinations show no defect in the structure and a solid joint. According to the microhardness values obtained in base metal, HAZ, and

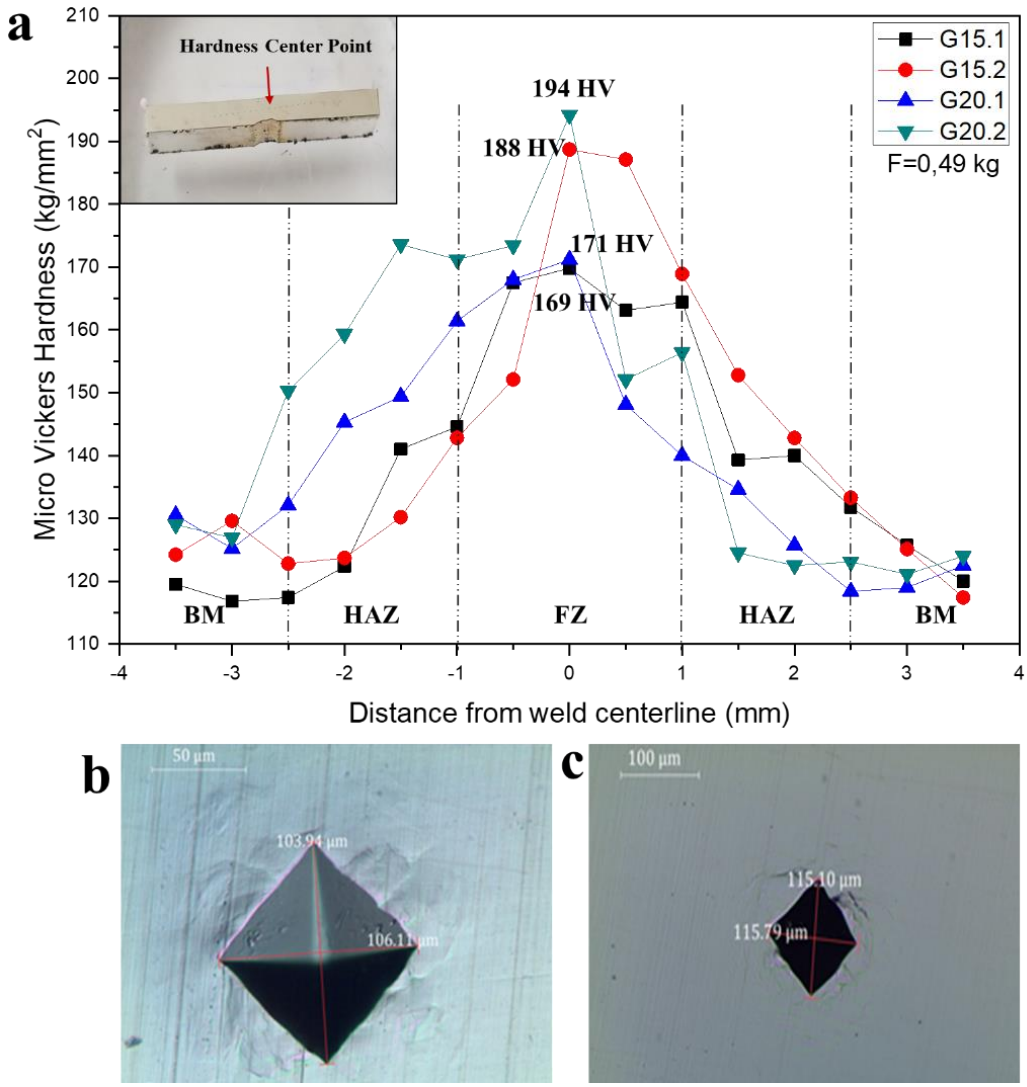

Figure 5. (a) Microhardness result graph of all samples, (b) Hardness trace measurement in the optical microscope of laser welded steel with a focal length of 15 mm, and (c) Hardness trace measurement of laser-welded steel optical microscope with a focal length of 20 mm.

fusion zone, laser welding of galvanized steel sheets does not soften HAZ. The fusion zone's hardness is about 1.5 times greater than that of the base metal due to the quick heating and cooling rate of laser welding, which also results in little lateral displacement of the welding joint. Furthermore, welding joints' hardness can be shielded from the effects of stress concentration by using quick heating and cooling rates. Figure 4 illustrates that the fusion zone's metallurgical structure is upperbainite + low-carbon martensite, whereas the HAZ's metallurgical structure is upperbainite + low-carbon martensite + ferrite. As low-carbon martensites exist, welding joints don't have a particularly high toughness. HAZ's greater hardness than base metal confirms that laser-welded galvanized steel sheets do not cause HAZ to become softer. This is attributed to the fact that the heating and cooling rates are fast enough during laser welding, and the incomplete annealed zone of HAZ is extremely narrow. Moreover, a certain amount of hardened layer is produced in HAZ during laser welding. The measurements of hardness distributions in the cross-section of welding joints have shown that the hardness in the fusion zone significantly increased compared with the base metal. As a result, it was determined that the hardness values of the weld zone increased compared to the base metal in all samples, and the hardness increased with the increase in focal length..

Conclusions

In the current study, the changes in microstructure and microhardness of galvanized steel plates joined by Nd: YAG laser welding were investigated. According to experimental findings, welding joints had greater strength and microhardness than the base metal. It was determined that a martensite structure was formed in the weld area due to rapid cooling, and therefore, the hardness value increased. As a result, the welding quality is trustworthy while producing metal components. It is possible to get joints free of pores and fractures under the circumstances of this experiment. The fusion zones exhibit incredibly high levels of grain refinement as a result of their rapid recrystallization and high welding rate, which raises the hardness of these areas relative to the base metal. SEM images revealed that there were no welding defects in the welding area of the sample combined with a focal length of 20 mm and that a successful process was carried out. In addition, EDS results also showed that zinc was removed from the metal due to high heat and cooling rates in the weld zone. This study showed that 2 mm thick galvanized plates can be successfully welded with a focal length of 20 mm. Thus, new laser welding parameters and their effects were introduced to literature and applications.

Declaration

The author(s) declared no potential conflicts of interest with respect to the research, authorship, and/or publication of this article. The author(s) also declared that this article is original and was prepared in accordance with international publication and research ethics, and ethical committee permission or any special permission is not required.

Author Contributions

A.K. Yontar and S. Çevik developed the methodology. Arife Kübra Yontar performed the analysis. S. Çevik supervised and improved the study. A.K. Yontar and S. Çevik wrote the manuscript together. A.K. Yontar and S. Çevik proofread the manuscript.

References

1. Wang B, Hu SJ, Sun L, Freiheit T. *Intelligent welding system technologies: State-of-the-art review and perspectives*. Journal of Manufacturing Systems 2020; **56**: p. 373–391.
2. Karayel E, Bozkurt Y. *Additive manufacturing method and different welding applications*. Journal of Materials Research and Technology 2020; **9** (5): p. 11424–11438.
3. Manh NH, van Nguyen A, Le Duy H et al. *Development of a novel GTAW process for joining ultra-thin metal sheets.* Journal of Manufacturing Processes 2022; **80** (2): p. 683–691.
4. Ebrahimpour A, Salami S, Saeid T. *Experimental and finite element investigation on hybrid GTAW-GMAW of duplex stainless steel*. International Journal Of Advanced Manufacturing Technology 2023; **125** (3-4): p. 1543–1557.
5. Weis S, Grunert R, Brumm S, Prank U. *Study on MIG-TIG hybrid brazing of galvanized thin sheet.* Weld World 2023; **67** (5): p. 1215–1221.
6. Azadi Moghaddam M, Kolahan F. *Modeling and optimization of A-GTAW process using back propagation neural network and heuristic algorithms*. International Journal of Pressure Vessels and Piping 2021; **194** (December): p. 104531.
7. Voigt AL, Cunha TVd, Niño CE. *Conception, implementation and evaluation of induction wire heating system applied to hot wire GTAW (IHW-GTAW)*. Journal of Materials Processing Technology 2020; **281** (2): p. 116615.
8. Sadeghian A, Iqbal N. *A review on dissimilar laser welding of steel-copper, steel-aluminum, aluminum-copper, and steel-nickel for electric vehicle battery manufacturing*. Optics & Laser Technology 2022; **146** (8): p. 107595.
9. Katayama S, Kawahito Y, Mizutani M. *Latest Progress in Performance and Understanding of Laser Welding*. Physics Procedia 2012; **39** (3): p. 8–16.
10. Wallerstein D, Salminen A, Lusquiños F et al. *Recent Developments in Laser Welding of Aluminum Alloys to Steel*. Metals 2021; **11** (4): p. 622.
11. Razmpoosh MH, Macwan A, Biro E, Zhou Y. *Effect of coating weight on fiber laser welding of Galvanneal-coated 22MnB5 press hardening steel*. Surface and Coatings Technology 2018; **337**: p. 536–543.

12. Chludzinski M, dos Santos RE, Churiaque C et al. *Pulsed Laser Welding Applied to Metallic Materials—A Material Approach*. Metals 2021; **11** (4): p. 640.
13. Mei L, Chen G, Jin X et al. *Research on laser welding of high-strength galvanized automobile steel sheets*. Optics and Lasers in Engineering 2009; **47** (11): p. 1117–1124.
14. Zhao Y, Zhang Y, Hu W, Lai X. *Optimization of laser welding thin-gage galvanized steel via response surface methodology*. Optics and Lasers in Engineering 2012; **50** (9): p. 1267–1273.
15. Murzin SP, Kazanskiy NL, Stiglbrunner C. *Analysis of the Advantages of Laser Processing of Aerospace Materials Using Diffractive Optics*. Metals 2021; **11** (6): p. 963.
16. Deepak JR, R.P A, Saran Sundar S. *Applications of lasers in industries and laser welding: A review*. Materials Today: Proceedings 2023.
17. Lun N, Saha DC, Macwan A et al. *Microstructure and mechanical properties of fibre laser welded medium manganese TRIP steel*. Materials & Design 2017; **131**: p. 450–459.
18. Thorpe SJ, Quinlan N, Ainsworth RW. *The characterisation and application of a pulsed neodymium YAG laser DGV system to a time-varying high-speed flow*. Optics & Laser Technology 2000; **32** (7-8): p. 543–555.
19. Liu B, Ohodnicki PR. *Fabrication and Application of Single Crystal Fiber: Review and Prospective*. Advanced Materials Technologies 2021; **6** (9): p. 5.
20. Schmidt M, Otto A, Kägeler C. *Analysis of YAG laser lap-welding of zinc coated steel sheets.* CIRP Annals 2008; **57** (1): p. 213–216.
21. Chakraborty A, Ghosh R, Sudan M, Mondal A. *Improvement in hot dip galvanized coating microstructure and properties by pre-metallic deposition on steel surface: A comprehensive review*. Surface and Coatings Technology 2022; **449**: p. 128972.
22. Autengruber R, Luckeneder G, Hassel AW. *Corrosion of press-hardened galvanized steel*. Corrosion Science 2012; 63: p. 12–19.
23. Dan A, Bijalwan PK, Pathak AS, Bhagat AN. *A review on physical vapor deposition-based metallic coatings on steel as an alternative to conventional galvanized coatings*. Journal of Coating Technology Research 2022; **19** (2): p. 403–438.
24. Kania H, Mendala J, Kozuba J, Saternus M. *Development of Bath Chemical Composition for Batch Hot-Dip Galvanizing-A Review*. Materials (Basel) 2020; **13** (18).
25. Zhang Z, Zhao Y, Wu S, Lu H. *Optimization of butt welding of zinc-coated thin sheets with oscillating fiber laser beams: Weld formation, microstructure, and mechanical properties.* Weld World 2021; **65** (9): p. 1711–1723.
26. Ma J, Kong F, Carlson B, Kovacevic R. *Two-pass laser welding of galvanized high-strength dual-phase steel for a zero-gap lap joint configuration*. Journal of Materials Processing Technology 2013; **213** (3): p. 495–507.
27. Sinha AK, Anand A. *Development of an alternative for corrosive resistant galvanized steel compatible for laser welding.* Materials Today: Proceedings 2021; **46** (11): p. 9561–9563.
28. Kim C, Choi W, Kim J, Rhee S. *Relationship between the Weldability and the Process Parameters for Laser-TIG Hybrid Welding of Galvanized Steel Sheets*. Materials Transactions 2008; **49** (1): p. 179–186.
29. Górka J, Suder W, Kciuk M, Stano S. *Assessment of the Laser Beam Welding of Galvanized Car Body Steel with an Additional Organic Protective Layer*. Materials (Basel) 2023; **16** (2).
30. Bang H-S, Kim J-C, Go B-S et al. *The Pre-Heating Effect for Porosity Control during the Laser Welding of Galvanized Steel Sheets.* Applied Sciences 2024; **14** (7): p. 2987.
31. Üren N. *Ecological dyeing and UV-protective functionalization of cotton/lyocell blend fabrics designed for high comfort summer clothing*. International Advanced Researches and Engineering Journal 2024; **8** (1): p. 43–50.
32. Sibillano T, Ancona A, Berardi V, Lugarà PM. *Correlation analysis in laser welding plasma*. Optics Communications 2005; **251** (1-3): p. 139–148.
33. Xia H, Tan C, Tian R et al. *Influence of shielding gas on microstructure and mechanical properties of laser welded–brazed Al/steel lapped joint*. Journal of Manufacturing Processes 2020; **54** (4): p. 347–358.
34. Hafez KM. *The influence of shielding gases on keyhole-induced porosity and nitrogen absorption in SS 304 stainless steel fiber laser welds*. International Journal of Advanced Manufacturing Technology 2023; **127** (3-4): p. 1887–1894.
35. Baghdadchi A, Hosseini VA, Hurtig K, Karlsson L. *Promoting austenite formation in laser welding of duplex stainless steel—impact of shielding gas and laser reheating*. Weld World 2021; **65** (3): p. 499–511.
36. Chung BG, Rhee S, Lee CH. *The effect of shielding gas types on CO2 laser tailored blank weldability of low carbon automotive galvanized steel*. Materials Science and Engineering: A 1999; 272 (2): p. 357–362.
37. Shreyas P, Panda B, Vishwanatha AD. *Characteristics of stainless steel-galvanized steel joint: Effect of stainless steel composition and welding parameters*. Materials Today: Proceedings 2019; **19** (1–4): p. 468–473.
38. Yontar AK, Çevik S. *Corrosion behavior of fiber laser welded Ti-6Al-4V alloy rods with different pH and temperature in 0.9 wt% NaCl medium*. Research on Engineering Structures and Materials 2024; ; **10** (2): p. 537-557
39. Liu H, Shui J, Cai T et al. *Microstructural evolution and hardness response in the laser beam welded joints of pure titanium during recrystallization and grain growth*. Materials Characterization 2018; **145**: p. 87–95.
40. Rong Z, Li L, Chen L et al. *The effect of Zn coating layer on the microstructure and mechanical properties of friction stir spot welded galvanized DP590 high-strength steel plates*. International Journal of Advanced Manufacturing Technology 2021; **113** (5-6): p. 1787–1798.
41. Betiku OT, Shojaee M, Sherepenko O et al. *Optimizing post-weld performance of press-hardened steel resistance spot welds by controlling fusion zone porosity*. Weld World 2022; **66** (9): p. 1733–1746.
42. Hao Y, Wang H-P, Sun Y et al. *The evaporation behavior of zinc and its effect on spattering in laser overlap welding of galvanized steels*. Journal of Materials Processing Technology 2022; **306** (9): p. 117625.

43. Hao Y, Chen N, Wang H-P et al. *Effect of zinc vapor forces on spattering in partial penetration laser welding of zinc-coated steels*. Journal of Materials Processing Technology 2021; **298** (part-A): p. 117282.
44. Kim H, Inoue J, Kasuya T. *Unsupervised microstructure segmentation by mimicking metallurgists' approach to pattern recognition*. Scientific Reports 2020; **10** (1): p. 17835.